Available online at www.sciencedirect.com
SCIENCE DIRECT®
International Journal of Thermal Sciences 42 (2003) 1073–1080
International Journal of Thermal Sciences
www.elsevier.com/locate/ijts

Effects of convection and inertia on close contact melting

Dominic Groulx *, Marcel Lacroix

Département de génie mécanique, Université de Sherbrooke, Sherbrooke, Québec, Canada J1K 2R1

Received 5 August 2002; accepted 6 March 2003

Abstract

An analytical study was conducted in order to examine the role of convection and inertia on close contact melting of a phase change material (PCM) resting on a sliding heated plate. Results indicate that for high Prandtl substances, inertia has no effect on contact melting regardless of the magnitude of the melt layer Reynolds number *Re*. Convection however, enhances contact melting and its effect is increasingly perceptible for $Re > 10^2$. Viscous dissipation may be ignored as long as $Re < 10^4$ and the Stefan number $Ste \geqslant 0.001$. On the other hand, for low Prandtl substances, both convection and inertia influence contact melting. Convection enhances melting while inertia hinders it. The effect of inertia is further accentuated as the Prandtl number becomes smaller. Viscous dissipation remains negligible as long as $Re < 10^6$ and $Ste \geqslant 0.001$.

1. Introduction

Close contact melting occurs when a solid melts while being in contact with a heat source. The liquid generated at the melting front is squeezed out from under the solid by the pressure maintained in the central section of the film by the weight of the free solid.

The problem of contact melting has been the subject of investigations related to the fundamentals of heat transfer [1–5], lubrication [6] and latent heat energy storage [7–9]. The importance of close contact melting lies in the fact that the heat flux across the thin melt layer separating the heated surface from the solid phase change material (PCM) is much higher than the heat transfer dominated by convection, which generally occurs in much thicker layers of molten material. As a result of the higher heat fluxes, the melting times are considerably reduced.

In most of the investigations reported in the open literature, the process by which the melt is squeezed out of the small gap separating the heat source and the solid is considered quasi-steady and the heat transfer through the liquid film is by conduction only [1–3,5–10]. This last assumption is however no longer valid when a relative motion between the solid and the heat source is imposed. In this case, convection heat transfer in the energy equation and inertia forces in the momentum equation must be taken into account in order to model faithfully the melting process.

Few studies have examined the effect of a relative motion between the PCM and the heated source on close contact melting [11,12]. These investigations focus on the transient thermal behaviour in the early stages of contact melting while conduction was still considered to be the prevailing mechanism of heat transfer across the melt layer. Convection was ignored.

The present paper overcomes this limitation by looking at the effects of both convection and inertia on close contact melting. These effects are delineated in terms of the Stefan and Reynolds numbers for high and low Prandtl substances. The assumptions of negligible viscous dissipation and of quasi steadiness of the melting process are also assessed.

2. Mathematical model

A schematic representation of the physical system is depicted in Fig. 1. A block of solid PCM of initial height H, length L and depth e initially at uniform melting temperature T_m rests on a flat plate. At time $t = 0$, the temperature of the flat plate is suddenly raised to a constant value $T_p = T_m + \Delta T$ and simultaneously a relative motion between the plate and the PCM is set. The amplitude of the relative motion is U. Melting is triggered and the solid descends vertically at a speed V while squeezing the melt out of the thin gap of thickness δ between the solid and the plate.

Five basic assumptions are made regarding the behaviour of the physical system:

* Corresponding author.

1290-0729/$ – see front matter
doi:10.1016/S1290-0729(03)00096-6

Nomenclature

C	heat capacity	$J{\cdot}kg^{-1}{\cdot}K^{-1}$
e	depth of the block	m
Ec	Eckert number, $= U^2/C_f\Delta T$	
g	acceleration of gravity	$m{\cdot}s^{-2}$
h	latent heat of fusion	$J{\cdot}kg^{-1}$
H	initial height of the block	m
k	thermal conductivity	$W{\cdot}m^{-1}{\cdot}K^{-1}$
L	length of the block	m
P	pressure	Pa
Pe	Peclet number, $= UL/\alpha$	
Pr	Prandtl number, $= \nu/\alpha$	
Q	flow rates	$m^2{\cdot}s^{-1}$
Re	Reynolds number, $= UL/\nu$	
S	molten height of the block	m
Ste	Stefan number, $= C_f\Delta T/h_{fs}$	
t	time	s
T	temperature	K
u	x velocity component	$m{\cdot}s^{-1}$
v	y velocity component	$m{\cdot}s^{-1}$
U	moving plate velocity	$m{\cdot}s^{-1}$
V	melting speed	$m{\cdot}s^{-1}$
x	coordinate	m
y	coordinate	m

Greek letters

α	thermal diffusivity of melt	$m^2{\cdot}s^{-1}$
δ	molten layer thickness	m
ΔT	temperature difference, $= T_p - T_m$	
ρ	density	$kg{\cdot}m^{-3}$
μ	dynamic viscosity	$N{\cdot}s{\cdot}m^2$
ν	kinematic viscosity	$m^2{\cdot}s^{-1}$

Subscripts

f	liquid
m	melting point
p	plate
s	solid
tot	total melt

Superscript

*	indicates dimensionless quantity

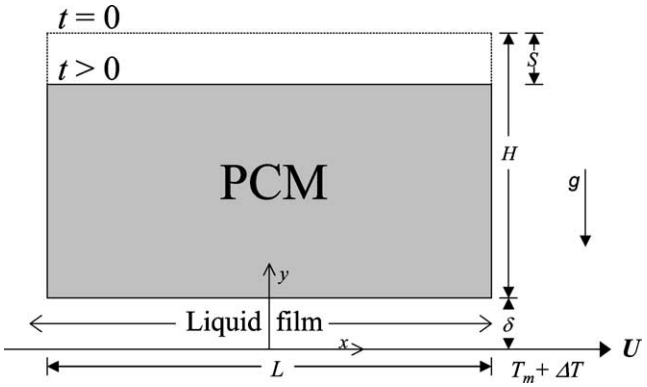

Fig. 1. Schematic of the system studied.

(1) The melting process is considered quasi-steady, i.e., at every point in time the weight of the solid is balanced by the excess pressure built in the liquid film;
(2) The transfer processes are one-dimensional (function of y only);
(3) The gap thickness δ is constant along the length L of the block (this assumption results from 2). The gap thickness δ may however vary with time;
(4) The flow in the liquid film remains laminar;
(5) The fluid properties are temperature independent.

2.1. Mass

Subjected to the above assumptions, the mass conservation equation for the melt is then:

$$\frac{\partial u}{\partial x} + \frac{\partial v}{\partial y} = 0 \tag{1}$$

Performing an order of magnitude analysis, one obtains the following result from Eq. (1):

$$v \approx U\frac{\delta}{L} \tag{2}$$

The vertical dimension of the thin melt gap δ is assumed very small in comparison with the length L of the block ($\delta \ll L$). It follows from Eq. (2) that the velocity v is negligibly small with respect to the velocity U of the moving plate.

2.2. Energy

The equation for the conservation of energy may be stated as:

$$u\frac{\partial T}{\partial x} + v\frac{\partial T}{\partial y} = \alpha_f\left(\frac{\partial^2 T}{\partial x^2} + \frac{\partial^2 T}{\partial y^2}\right) + \frac{\mu_f}{\rho_f C_f}\Phi \tag{3}$$

The last term on the right-hand side of Eq. (3) represents the effect of internal heat generation by fluid friction. An order of magnitude analysis of Eq. (3) yields the following result:

$$U\frac{\Delta T}{L} \approx \alpha_f\left(\frac{\Delta T}{L^2} + \frac{\Delta T}{\delta^2}\right) + \frac{\mu_f}{\rho_f C_f}\left(\frac{U}{\delta}\right)^2 \tag{4}$$

The diffusion term in the horizontal direction ($\Delta T/L^2$) can be neglected with respect to the diffusion term in the vertical direction ($\Delta T/\delta^2$). As a result, the effect

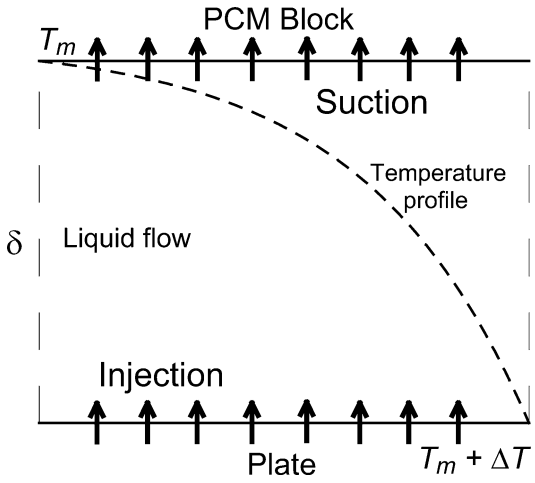

Fig. 2. Physical representation of the injection–suction theoretical model.

of convection is negligibly small with respect to that of conduction if

$$\left(\frac{\delta}{L}\right)^2 Pe \ll 1 \tag{5}$$

and the effect of viscous dissipation can be ignored in comparison to that of conduction if

$$Pr \cdot Ec \ll 1 \tag{6}$$

For most of the cases examined in this study, Eq. (6) is satisfied. The effect of convection must however be retained when a relative motion is set between the heated plate and the PCM block. For a one-dimensional transfer process, Eq. (3) then becomes:

$$U\frac{\delta}{L}\frac{\mathrm{d}T}{\mathrm{d}y} = \alpha_f \frac{\mathrm{d}^2T}{\mathrm{d}y^2} \tag{7}$$

with $T(y=0) = T_p = T_m + \Delta T$ and $T(y=\delta) = T_m$ as the boundary conditions. The additional assumption that the problem can still be accurately modelled in one dimension (vertical direction) has been made and Eq. (2) was used to replace v in Eq. (7).

Eq. (7) is the energy equation retained in the present model. From a physical point of view, modelling the effect of convection may be pictured as the injection of warm fluid through the plate at a speed $v = U\delta/L$ and suction of the same amount of cold fluid through the PCM block at the same speed (Fig. 2). As a result, the heat flux at the surface of the PCM block is larger than that at the surface of the heated plate and energy is conserved via the injection and the suction of fluid in the melt gap.

The temperature profile in the liquid gap is then given by:

$$T(y) = T_m + \Delta T \frac{\{\exp(U\delta y/\alpha_f L) - \exp(U\delta^2/\alpha_f L)\}}{1 - \exp(U\delta^2/\alpha_f L)} \tag{8}$$

This temperature, depicted in Fig. 3, shows that the effect of convection becomes increasingly important as $(\delta/L)^2 Pe$ augments. For $(\delta/L)^2 Pe > 0.1$, the temperature profile

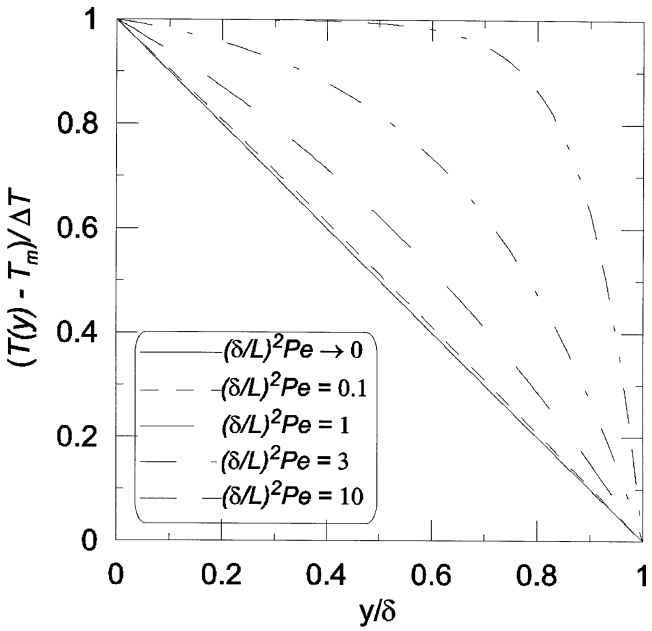

Fig. 3. Temperature profile in the melt gap as a function of y.

departs from the linear distribution found in the case of no relative motion between the PCM block and the heated plate.

The relation between the gap thickness and the melting speed follows from an energy balance at the melting interface ($y = \delta$), i.e.:

$$-k_f\left(\frac{\mathrm{d}T}{\mathrm{d}y}\right)_{y=\delta} = h_{fs}\rho_s V \tag{9}$$

Substituting Eq. (8) in Eq. (9) provides a first relation between the molten layer thickness δ and the melting speed V:

$$-\rho_f C_f \frac{U\delta\Delta T}{L}\frac{1}{\exp(-U\delta^2/\alpha_f L) - 1} = h_{fs}\rho_s V \tag{10}$$

2.3. Momentum

At all times, it is assumed that the pressure in the liquid gap is related to the weight of the PCM block by:

$$e\int_{-L/2}^{L/2} P(x)\,\mathrm{d}x = \rho_s(H - S)eLg \tag{11}$$

From the momentum conservation equation in the horizontal direction,

$$u\frac{\partial u}{\partial x} + v\frac{\partial u}{\partial y} = \frac{-1}{\rho_f}\frac{\mathrm{d}P}{\mathrm{d}x} + \nu_f\left(\frac{\partial^2 u}{\partial x^2} + \frac{\partial^2 u}{\partial y^2}\right) \tag{12}$$

it is found that

$$\frac{U^2}{L} \approx -\frac{1}{\rho_f}\frac{\mathrm{d}P}{\mathrm{d}x} + \nu_f\left(\frac{U}{L^2} + \frac{U}{\delta^2}\right) \tag{13}$$

where (U/L^2) is negligibly small with respect to (U/δ^2). Inertia may be neglected with respect to friction if the following condition is satisfied:

$$\left(\frac{\delta}{L}\right)^2 Re \ll 1 \tag{14}$$

The effect of the inertia forces cannot, however, be discarded automatically when the plate is set in motion. As a result, the momentum conservation equation retained here becomes, for a one dimensional process:

$$U\frac{\delta}{L}\frac{\mathrm{d}u}{\mathrm{d}y} = -\frac{1}{\rho_f}\frac{\mathrm{d}P}{\mathrm{d}x} + \nu_f\frac{\mathrm{d}^2u}{\mathrm{d}y^2} \tag{15}$$

with $U(y=0)=U$ and $U(y=\delta)=0$ for the boundary conditions. As for the energy conservation Eq. (7), Eq. (15) may be viewed as a combination of injection and suction of mass in the melt gap. Further details on this approach may be found in reference [13].

Substituting Eq. (2) for v in Eq. (15) and solving yields the following velocity profile:

$$u(x,y) = -\frac{\nu_f L P_x}{U\delta}y + \frac{(U - \frac{\nu_f L P_x}{U})}{1-\exp(\frac{U\delta^2}{\nu_f L})}\exp\left(\frac{U\delta}{\nu_f L}y\right) + \frac{(\frac{\nu_f L P_x}{U} - U\exp(\frac{U\delta^2}{\nu_f L}))}{1-\exp(\frac{U\delta^2}{\nu_f L})} \tag{16}$$

where

$$P_x = \frac{1}{\mu_f}\frac{\mathrm{d}P}{\mathrm{d}x}$$

From the definition of the height integrated flow rate,

$$Q(x) = \int_0^\delta u(x,y)\,\mathrm{d}y \tag{17}$$

and with the help of Eq. (16), it is possible to calculate the mass flow rate. Integration of Eq. (1) from $y=0$ $(v=0)$ to $y=\delta$ $(v=-V)$ yields,

$$\frac{\mathrm{d}Q(x)}{\mathrm{d}x} = V \tag{18}$$

Differentiating the result obtained in Eq. (17), the following relation between the pressure and the melting speed is obtained:

$$V = \frac{\mathrm{d}^2P}{\mathrm{d}x^2}(\xi) = \xi\frac{\mathrm{d}^2P}{\mathrm{d}x^2} \tag{19}$$

where

$$\xi = \left(\frac{\mu_f L^2}{\rho_f^2 U^2\delta} - \frac{L\delta}{2U\rho_f} + \frac{\frac{L\delta}{U\rho_f}}{1-\exp(\frac{U\delta^2}{\nu_f L})}\right)$$

Integrating Eq. (19) twice with respect to x and using the boundary conditions for the pressure $P(x=\pm L/2)=0$, one obtains:

$$P(x) = \frac{V}{8\xi}\left(4x^2 - L^2\right) \tag{20}$$

Table 1
Dimensionless variables and parameters

δ^*	δ/L
H^*	H/L
S^*	S/L
V^*	VL/ν_f
ρ^*	ρ_s/ρ_f
T^*	$\nu_f t/L^2$
A	L^3g/ν_f^2

Table 2
Dimensionless numbers

Ste	$C_f\Delta T/h_{fs}$
Re	UL/ν_f
Pr	ν_f/α_f
Re	UL/ν_f

Substitution of Eq. (20) in Eq. (11) provides a second relation between the molten layer thickness δ and the melting speed V:

$$-\frac{VL^2}{12\xi} = \rho_s(H-S)g \tag{21}$$

2.4. Dimensionless equations

Eqs. (10) and (21) were cast in dimensionless form using the variables and parameters defined in Table 1 and three dimensionless numbers provided in Table 2:

$$-\frac{\delta^*}{\exp(-Re\,Pr\,\delta^{*2})-1}Ste\,Re = \rho^*V^* \tag{22}$$

$$-\frac{V^*Re}{12\xi^*} = \rho^*(H^*-S^*)A \tag{23}$$

with

$$\xi^* = \frac{1}{Re\,\delta^*} - \delta^*\left(\frac{1}{2} + \frac{1}{\exp(Re\,\delta^{*2})-1}\right).$$

The Prandtl number *Pr* characterises the substance, the Stefan number *Ste* the heating intensity and the Reynolds number *Re* the magnitude of the relative motion between the heated plate and the PCM block. The Peclet and Eckert numbers are defined in the nomenclature.

Both Eqs. (22) and (23) are nonlinear equations for V^* and δ^*. Their numerical solution is obtained from a regula falsa method. The total melting time may then be extracted from the solution for δ^*.

3. Results and discussion

Eqs. (22) and (23) were solved numerically. Different melting scenarios $(0.0001 \leqslant Ste \leqslant 1)$ and different rela-

Table 3
Thermo physical properties of *n*-octadecane

ρ_f	776 kg·m^{-3}
ρ_s	814 kg·m^{-3}
C	2240 J·kg^{-1}·K^{-1}
k	0.152 W·m^{-1}·K^{-1}
ν	4.639×10^{-6} m^2·s^{-1}
α	8.75×10^{-8} m^2·s^{-1}
h	242×10^3 J·kg^{-1}
Pr	57

Table 4
Thermo physical properties of gallium

ρ	6094.7 kg·m^{-3}
C	398 J·kg^{-1}·K^{-1}
k	33.49 W·m^{-1}·K^{-1}
ν	2.87×10^{-7} m^2·s^{-1}
α	1.3667×10^{-5} m^2·s^{-1}
h	80 160 J·kg^{-1}
Pr	0.0208

Table 5
Thermo physical properties of potassium (Temperature = 350 K)

ρ_f	824.4 kg·m^{-3}
ρ_s	860 kg·m^{-3}
C	818 J·kg^{-1}·K^{-1}
k	54.2 W·m^{-1}·K^{-1}
ν	6.28×10^{-7} m^2·s^{-1}
α	8.037×10^{-5} m^2·s^{-1}
h	2 330 J·kg^{-1}
Pr	0.00782

tive motion between the heated plate and the PCM block ($0 \leqslant Re \leqslant 10^6$) were examined. Three substances were considered: *n*-octadecane ($Pr = 57$), gallium ($Pr = 0.0208$) and potassium ($Pr = 0.00782$). Their thermo physical properties are provided in Tables 3, 4 and 5, respectively. For all simulations reported here, the initial dimensions of the PCM block are $L = 0.1$ m and $H = 0.1$ m (Fig. 1).

3.1. High-Pr substances

Fig. 4 shows the temporal variation of the thickness of a PCM block ($H^* - S^*$) made of *n*-octadecane ($Pr = 57$), for Reynolds numbers varying from 0 to 1.75×10^4. The Stefan number is maintained equal to 0.1. As time passes, the PCM block melts and the thickness ($H^* - S^*$) diminishes. It is seen that the effect of the relative motion on the melting process remains imperceptible for $Re \leqslant 10^2$. For $Re > 10^2$ however, convection in the melt layer enhances melting and dominates for $Re \geqslant 10^4$. It was also found that simulations conducted with and without the inertia term in the momentum equation (15) yield the same results. Inertia appears to play an insignificant role in the contact melting of high-*Pr* substances.

Another interesting feature of Fig. 4 is that, for $Re < 10^4$, the melting rate (or speed V) decreases as the block melts and increases for $Re \geqslant 10^4$. The effect of convection on contact melting is further exemplified by the temporal variation of the Nusselt number at the solid–liquid interface (Fig. 5). The Nusselt number, Nu_L , is defined as:

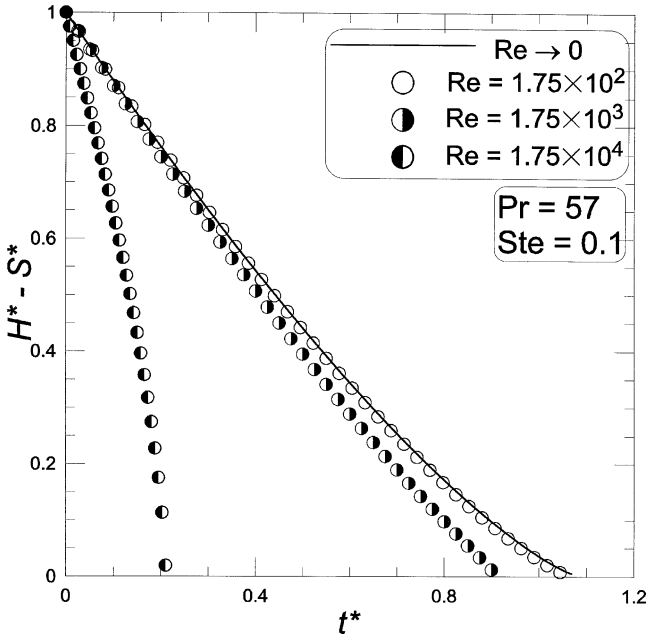

Fig. 4. $H^* - S^*$ versus t^* for $Pr = 57$ at $Ste = 0.1$.

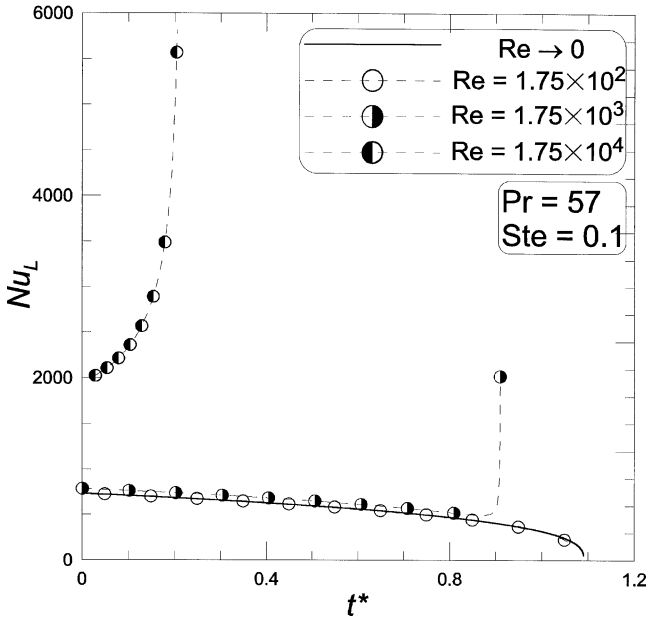

Fig. 5. Nu_L versus t^* for $Pr = 57$ at $Ste = 0.1$.

$$Nu_L = \frac{q''}{k_f \Delta T / L} = -\frac{\mathrm{d}T/\mathrm{d}y|_{y=\delta}}{\Delta T / L} \tag{24}$$

The melting speed V^* is linked to the Nusselt number via the following expression:

$$V^* = \frac{Ste}{\rho^* Pr} Nu_L \tag{25}$$

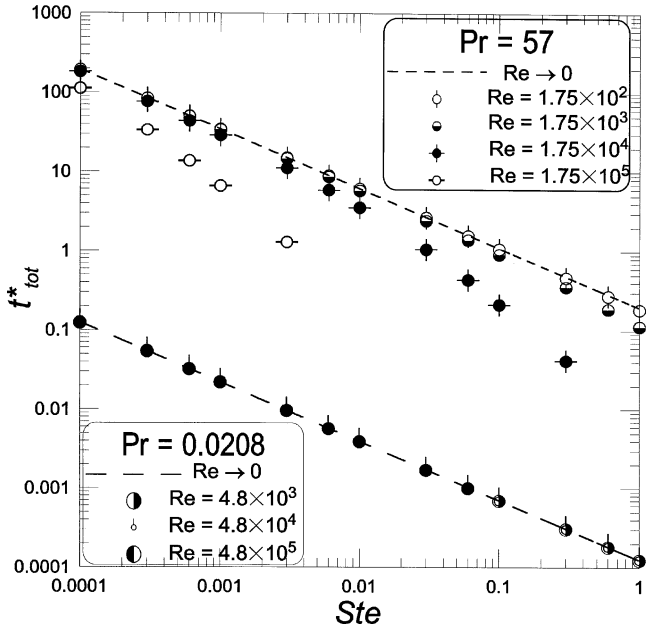

Fig. 6. Total melting time (t^*_{tot}) versus *Ste* for *n*-octadecane and gallium.

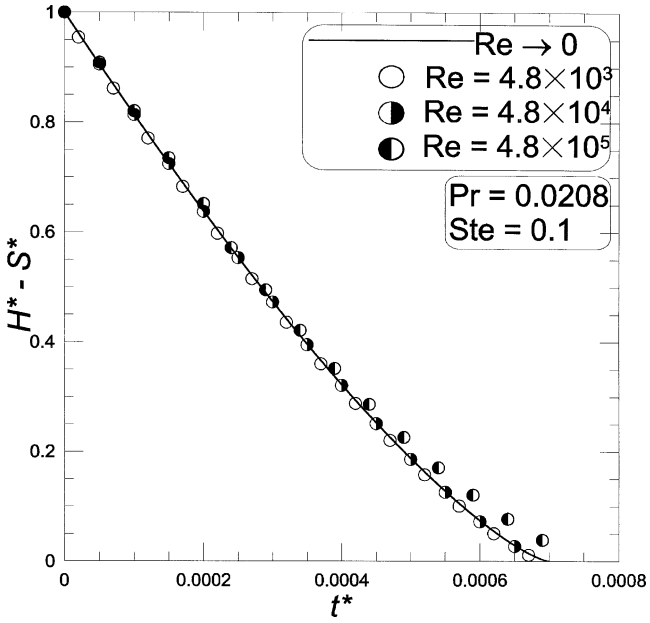

Fig. 7. $H^* - S^*$ versus t^* for $Pr = 0.0208$ at $Ste = 0.1$.

Comparison of Figs. 4 and 5 reveals that, for $Re < 10^4$, the time wise Nusselt number decreases in the same manner as the melting speed. Its magnitude remains slightly larger than that for the case of no relative motion between the PCM block and the heated plate ($Re \to 0$). For $Re \geqslant 10^4$ however, convection dominates the melting process and the temporal variation of the Nusselt number is radically different. Not only is the magnitude of the Nusselt number larger but it increases steeply, like the melting speed (Eq. 25), as time passes.

The variation of the dimensionless melting time t^*_{tot}, that is the time needed to melt entirely the PCM block, with respect to *Ste* is depicted in Fig. 6 for *n*-octadecane and for gallium ($Pr = 0.0208$). For *n*-octadecane, it is seen that t^*_{tot} decreases linearly with *Ste* and it remains independent of the relative motion for $Re \leqslant 10^2$. For $Re > 10^2$ however, t^*_{tot} versus *Ste* departs form a linear relation. The melting time diminishes and the decrease is accentuated as the Stefan number increases.

3.2. Low-Pr substances

The temporal variation of $(H^* - S^*)$ for a low-*Pr* substance, i.e., gallium ($Pr = 0.0208$), is depicted in Fig. 7. The Stefan number is kept constant ($Ste = 0.1$) and the Reynolds number varies from 0 to 4.8×10^5. Contrary to high-*Pr* substances, the effect of convection on contact melting of low-*Pr* substances remains negligible for $Re < 5.0 \times 10^4$. For $Re > 10^5$ however, the melting rate slows down! This behaviour is further accentuated for lower Pr substances such as potassium (Fig. 8). It is the result of the inertia forces acting on the flow (Eq. 15).

Fig. 9 distinguishes the effects of inertia and of convection on the melting of potassium for a given test case

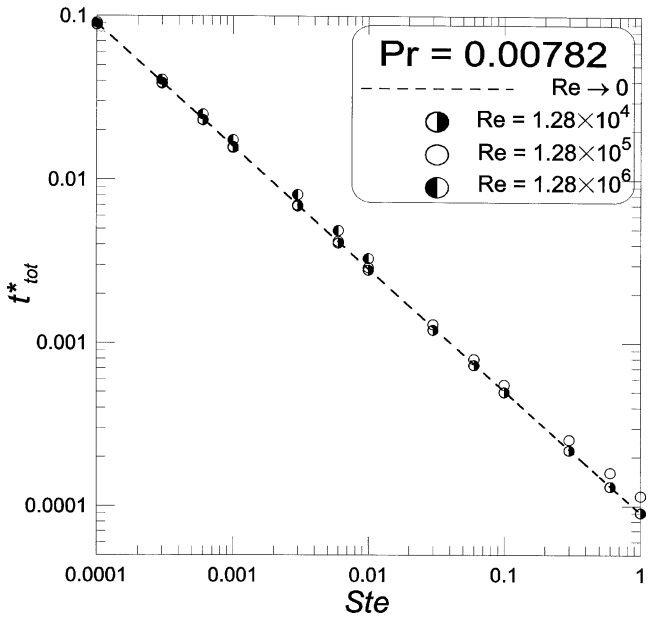

Fig. 8. Total melting time (t^*_{tot}) versus *Ste* for potassium.

($Re = 1.28 \times 10^5$ and $Ste = 0.3$). It is clear that convection enhances melting while inertia hinders it. Both effects must however be taken into account simultaneously when simulating contact melting of low-*Pr* substances.

3.3. Limitations of the model

In closing the discussion, some of the limitations of the above mathematical model must be stressed.

The first limitation concerns the effect of viscous dissipation. This effect is negligible provided that Eq. (6) is satisfied. Fig. 10 shows that viscous dissipation may be ignored

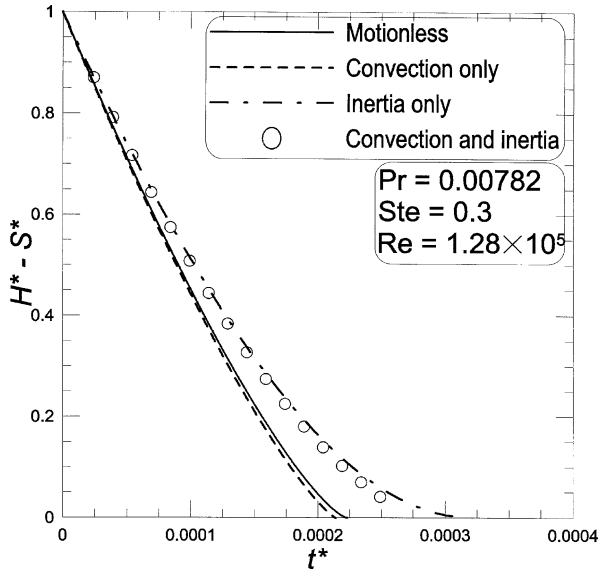

Fig. 9. $H^* - S^*$ versus t^* for $Pr = 0.00782$, $Ste = 0.3$ and $Re = 1.28 \times 10^5$.

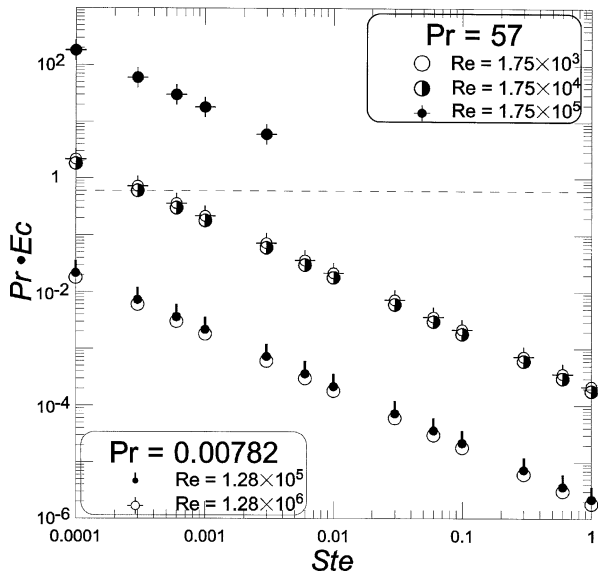

Fig. 10. Viscous heating versus Stefan number.

for high-Pr substances when $Re < 10^4$ and $Ste \geqslant 0.001$. For low-Pr substances, viscous dissipation remains negligible as long as $Re < 10^6$ and $Ste \geqslant 0.001$.

The second limitation concerns the quasi steadiness of the contact melting process. For high Reynolds number ($Re > 10^6$), the static equilibrium between the dimensionless pressure in the liquid layer and the dimensionless weight of the PCM block above may, at some point in time, break down. Then, the set of Eqs. (22), (23) no longer has a solution. An example is provided in Fig. 11, for $Pr = 0.00782$, $Ste = 0.06$ and $Re = 1.28 \times 10^6$. At approximately $t^* \approx 3.25 \times 10^{-4}$, 40% of the PCM block has melted. The pressure in the melt layer no longer balances the weight of the block and Eqs. (22), (23) diverge quickly. The temporal

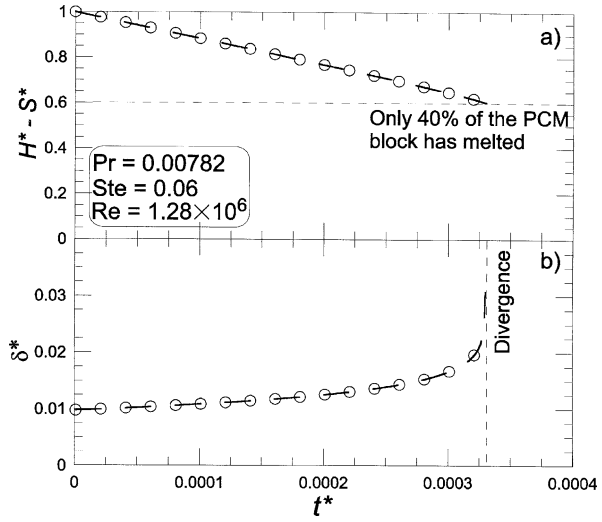

Fig. 11. Case where the quasi-steady assumption is not satisfied: $Pr = 0.00782$, $Ste = 0.06$ and $Re = 1.28 \times 10^6$; (a) $H^* - S^*$ versus t^*; (b) δ^* versus t^*.

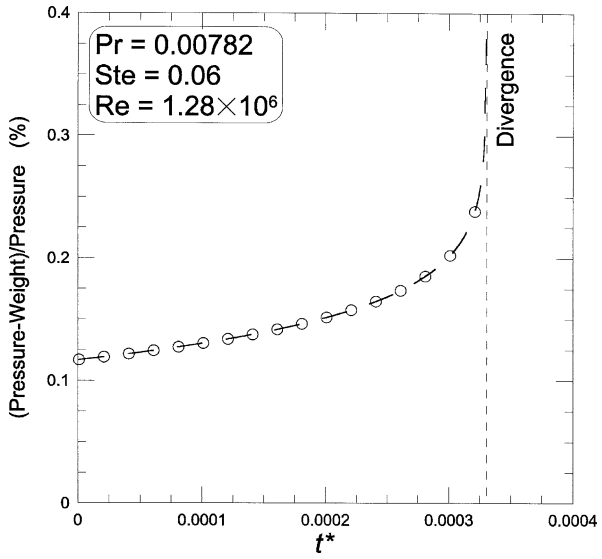

Fig. 12. Relative error between pressure and weight versus t^*.

discrepancy between the pressure and the weight is clearly illustrated in Fig. 12.

4. Concluding remarks

A numerical study was conducted to examine the role of convection and of inertia on close contact melting of a phase change material resting on a sliding heated plate. Based on the results obtained, the main conclusions are summarised below.

- For high-Pr substances, inertia has no effect on contact melting regardless of the magnitude of the melt layer Reynolds number Re . Convection however, enhances contact melting. Its effect is increasingly perceptible for $Re > 10^2$;

- For low-*Pr* substances, both convection and inertia influence contact melting. Convection enhances melting while inertia hinders it. The effect of inertia is further accentuated as the *Pr* number becomes smaller. For $Pr \leqslant 0.01$ and $Re \geqslant 10^4$, the relative motion between the PCM and the heated plate slows down the melting process;
- For high-*Pr* substances, viscous dissipation may be ignored as long as $Re < 10^4$ and $Ste \geqslant 0.001$;
- For low-*Pr* substances, viscous dissipation remains negligible as long as $Re < 10^6$ and $Ste \geqslant 0.001$;
- For $Re \geqslant 10^6$, the assumption of quasi steadiness of the melting process in the model may become invalid. In this case, the pressure in the melt layer no longer balances the weight of the PCM block and the numerical solution of the conservation equations diverges.

Results reported here rest on an order of magnitude analysis. Moreover, the mathematical model assumes (Assumption 2) that the transfer processes are one-dimensional only. When the relative motion between the heated plate and the PCM block becomes important, i.e., for $Re \approx 10^4$ and higher, this assumption is no longer valid. The thickness of the melt gap varies in the x direction. In this case, a more complex two-dimensional transfer model would be more suitable for capturing the physics underlying the contact melting process. The present study has paved the way to the development of such a model.

Acknowledgements

The authors are grateful to the Natural Sciences and Engineering Research council of Canada and to the Fonds Québécois de la Recherche sur la nature et les technologies for their financial support.

References

[1] M. Lacroix, Contact melting of a phase change material inside a heated parallelepipedic capsule, Energy Conversion Management 42 (2001) 35–47.
[2] M.K. Moallemi, B.W. Webb, R. Viskanta, An experimental and analytical study of close-contact melting, J. Heat Transfer 108 (1986) 894–899.
[3] A. Saito, H. Hong, O. Hirokane, Heat transfer enhancement in the direct contact melting process, Internat. J. Heat Mass Transfer 35 (1992) 295–305.
[4] H. Hong, A. Saito, Numerical method for direct contact melting in transient process, Internat. Heat Mass Transfer 36 (1993) 2093–2103.
[5] M. Bareiss, H. Beer, An analytical solution of the heat transfer process during melting of an unfixed solid phase change material inside a horizontal tube, Internat. J. Heat Mass Transfer 27 (1984) 739–745.
[6] A. Bejan, Contact melting heat transfer and lubrication, Adv. Heat Transfer 24 (1994) 1–38.
[7] S.K. Roy, S. Sengupta, The melting process within spherical enclosures, J. Heat Transfer 109 (1987) 460–462.
[8] T. Hirata, Y. Makino, Y. Kaneko, Analysis of close-contact melting for octadecane and ice inside isothermally heated horizontal rectangular capsule, Internat. J. Heat Mass Transfer 34 (1991) 3091–3106.
[9] W.Z. Chen, S.M. Cheng, Z. Luo, W.M. Gu, Analysis of contact melting of phase change materials inside a heated rectangular capsule, Internat. J. Energy Res. 19 (1995) 337–345.
[10] A. Bejan, Convection Heat Transfer, Wiley, New York, 1995.
[11] H. Yoo, Analytical solutions to unsteady close-contact melting on a flat plate, Internat. J. Heat Mass Transfer 43 (2000) 1457–1467.
[12] H. Yoo, Initial transient behaviour during close-contact melting induced by convective heating, Internat. J. Heat Mass Transfer 44 (2001) 2193–2197.
[13] F.M. White, Viscous Fluid Flow, McGraw-Hill, New York, 1991.